

A Comprehensive Study of Disordered and Ordered Scheelite-Related $\text{Bi}_3(\text{FeO}_4)(\text{MoO}_4)_2$

By W. JEITSCHKO,* A. W. SLEIGHT, W. R. MCCLELLAN AND J. F. WEIHER

Central Research and Development Department,† E. I. du Pont de Nemours and Company,
Wilmington, Delaware 19898, U.S.A.

(Received 14 July 1975; accepted 22 September 1975)

$\text{Bi}_3(\text{FeO}_4)(\text{MoO}_4)_2$, prepared from aqueous solutions of the components, is microcrystalline and has $I4_1/a$ scheelite-type structure ($a=5.32$, $c=11.67$ Å) with a random distribution of the Fe and Mo atoms on the tetrahedral cation site. This phase is metastable and transforms on heating to an ordered scheelite superstructure: $C2/c$, $a=16.904$, $b=11.653$, $c=5.254$ Å, $\beta=107.15^\circ$; $Z=4$. The structure was solved and refined from single-crystal counter data: $R=0.061$ for 1083 structure factors. Both crystallographically different Bi atoms show lone-pair distortions. The Fe and Mo atoms are tetrahedrally coordinated to O atoms. Strong Bi–O bonds result in unusually long Fe–O distances which correlate well with a large isomer shift of 0.282 mm s^{-1} relative to $\alpha\text{-Fe}$ for tetrahedral Fe^{3+} in the ^{57}Fe Mössbauer spectrum. The Mössbauer data also indicate a trend towards higher coordination of the Fe atom in the disordered phase. Infrared spectra suggest considerable short-range disorder in that phase. $\text{Bi}_3(\text{GaO}_4)(\text{MoO}_4)_2$ forms disordered and ordered scheelite phases isotypic with $\text{Bi}_3(\text{FeO}_4)(\text{MoO}_4)_2$. Scheelite-related phases are classified according to their group-subgroup relationships. Scheelite-related YNbO_4 which was previously reported with a noncentrosymmetric space group appears to be centrosymmetric.

Introduction

Of the crystal structures occurring for ABO_4 compounds, the scheelite (CaWO_4) type structure is the most versatile. It is adoptable for a large range of radii ratios and charge combinations of the cations (Muller & Roy, 1974). Ordering of vacancies and cations on the A site gives rise to various superstructures as is known for the $\text{Eu}_{2/3}\square_{1/3}\text{WO}_4$ (Templeton & Zalkin, 1963), $\text{Bi}_{2/3}\square_{1/3}\text{MoO}_4$ (Cesari, Perego, Zazzetta, Manara & Notari, 1971; van den Elzen & Rieck, 1973), and $\text{La}_{2/3}\square_{1/3}\text{MoO}_4$ (Brixner, Sleight & Lics, 1972; Jeitschko, 1973) type structures, where \square indicates vacant sites. A superstructure due to ordering of two kinds of cations on the A site was reported for $\text{KEu}(\text{MoO}_4)_2$ (Klevtsova, Kozeeva & Klevtsov, 1974). In $\text{Bi}_3(\text{FeO}_4)(\text{MoO}_4)_2$ the formation of a superstructure was ascribed (Sleight & Jeitschko, 1974) to ordering of the Fe and Mo atoms on the B site of scheelite. Here we give a detailed characterization of this phase which is of interest also because of its catalytic properties (Linn & Sleight, 1976).

Synthesis and polymorphism

The synthesis of $\text{Bi}_3(\text{FeO}_4)(\text{MoO}_4)_2$ is most convenient from aqueous solutions of ferric nitrate, bismuth nitrate, and ammonium molybdate (Sleight & Jeitschko, 1974). If this mixture is heated to only 250°C to drive off the ammonium nitrate and water, a new modification of $\text{Bi}_3(\text{FeO}_4)(\text{MoO}_4)_2$ is formed, which gives the X-ray powder pattern shown in Fig. 1(a). We will refer to this modification as disordered $\text{Bi}_3(\text{FeO}_4)(\text{MoO}_4)_2$

since its powder pattern contains the basic scheelite-type reflections without superstructure reflections. The peaks are broad and can be indexed on the basis of a body centered tetragonal cell with $a=5.32$ and $c=11.67$ Å.

The X-ray powder pattern of the modification we have previously described is also characteristic of a scheelite structure, but there is line splitting and a superstructure [Fig. 1(b)]. We refer to this phase as ordered $\text{Bi}_3(\text{FeO}_4)(\text{MoO}_4)_2$.

The diffraction peaks of the disordered phase are broad, but not as broad as the splitting in the ordered form [compare for instance the 200 reflection in Fig. 1(a) with 640 and $20\bar{2}$ reflections in Fig. 1(b)]. Since even the 004 reflection – which does not split in the ordered form – is broad, the broadening can at least to a large extent be ascribed to the small crystallite size. Excluding lattice distortions and inhomogeneities as cause for the broadening, the crystallite size was calculated with the Scherrer formula to be about 250 Å. Annealing experiments showed that weak superstructure reflections occur as soon as the scheelite reflections begin to sharpen. Thus crystal growth and the ordering process occur at similar conditions.

If disordered $\text{Bi}_3(\text{FeO}_4)(\text{MoO}_4)_2$ is heated at 600° to 920°C for 10 h, it completely transforms to ordered $\text{Bi}_3(\text{FeO}_4)(\text{MoO}_4)_2$. Heating disordered $\text{Bi}_3(\text{FeO}_4)(\text{MoO}_4)_2$ at 500°C for 10 h leads to no significant sharpening of the diffraction peaks and no detectable formation of ordered $\text{Bi}_3(\text{FeO}_4)(\text{MoO}_4)_2$. However, when disordered $\text{Bi}_3(\text{FeO}_4)(\text{MoO}_4)_2$ was used in a catalytic reactor for several days, it completely transformed to ordered $\text{Bi}_3(\text{FeO}_4)(\text{MoO}_4)_2$ even though the temperature never exceeded 475°C . Thus, disordered $\text{Bi}_3(\text{FeO}_4)(\text{MoO}_4)_2$ is metastable. Nonetheless, it is kinetically fairly stable up to about 500°C . Dis-

* Present address: University of Giessen, 63 Giessen, West Germany.

† Contribution No. 2287.

ordered $\text{Bi}_3(\text{FeO}_4)(\text{MoO}_4)_2$ could be expected to be thermodynamically stable at high temperatures; however, the compound melts incongruently at 925°C (DTA data show an endotherm on heating at this temperature and quenching from above that temperature gives a multiple phase product).

The colors of the two $\text{Bi}_3(\text{FeO}_4)(\text{MoO}_4)_2$ phases are different. In samples with small particle size the disordered form is light brown and the ordered form greenish yellow. Prolonged sintering and grain growth of the ordered form, however, result in a dark brown color.

Crystal structure of ordered $\text{Bi}_3(\text{FeO}_4)(\text{MoO}_4)_2$

Small crystals of ordered $\text{Bi}_3(\text{FeO}_4)(\text{MoO}_4)_2$ were obtained by sintering at 920°C for about 60 h in air. They were investigated in a Buerger precession camera with $\text{Mo K}\alpha$ radiation and show $2/m$ diffraction symmetry. Extinctions (hkl present only with $h+k=2n$; $h0l$ only with $l=2n$) indicate space groups $C2/c$ and Cc ; $C2/c$ was found to be correct during the structure determination. This is also supported by the absence of a second harmonic signal in isostructural $\text{Bi}_3(\text{GaO}_4)(\text{MoO}_4)_2$.

Lattice constants were obtained from a least-squares refinement of Hagg-Guinier data recorded at 25°C using $\text{Cu K}\alpha_1$ radiation with high-purity KCl ($a=6.2931 \text{ \AA}$) as internal standard: $a=16.904$ (1) $b=11.653$ (1), $c=5.2544$ (6) \AA , $\beta=107.15$ (1) $^\circ$, $V=989.0$ (1) \AA^3 . The values given in parentheses are standard deviations in the least significant digits; they do not reflect any compositional variation in lattice constants. The calculated density is 7.16 g cm^{-3} assuming four formula units per cell.

Intensity data

The crystal selected for the collection of the intensity data was of irregular shape with overall extensions varying between 35 and 65 μm . Zr-filtered Mo radiation was used with a four-circle automated diffractometer, scintillation counter, and pulse-height discriminator. Scans were over 0.8° in 2θ plus the angular separation of the $\text{K}\alpha$ doublet with scan speed of $0.2^\circ 2\theta \text{ min}^{-1}$. Background was counted for 40 s at both ends of each scan. All reflections within three asymmetric quadrants up to $65^\circ 2\theta$ were measured. Equivalent reflections were averaged. An absorption correction was made assuming spherical crystal shape [$\mu(\text{Mo K}\alpha)=549 \text{ cm}^{-1}$, $\mu_r=1.3$; Weber, 1969]. The usual Lorentz-polarization correction was applied.

Solution and refinement of the structure

Fig. 2. shows the relation of the tetragonal scheelite cell* to that of $\text{Bi}_3(\text{FeO}_4)(\text{MoO}_4)_2$. We expected that

* We use the standard setting $C2/c$ for $\text{Bi}_3(\text{FeO}_4)(\text{MoO}_4)_2$. The relation of the scheelite cell to the $\text{Bi}_3(\text{FeO}_4)(\text{MoO}_4)_2$ cell is more easily recognized in the $I2/a$ setting. The lattice constants for the $I2/a$ cell are $a=5.254$, $b=11.653$, $c=16.155 \text{ \AA}$, $\beta=90.96^\circ$.

the superstructure arises through ordering of the Fe and Mo atoms on the B site of the ABO_4 scheelite structure. Since the point symmetry of the B site is noncentric, only the $4(e)$ position of $C2/c$ is suited for the four Fe atoms in $\text{Bi}_3(\text{FeO}_4)(\text{MoO}_4)_2$. The remaining atoms were then placed according to the positions of the subcell.

The structure was refined with a full-matrix least-squares program by Finger (1969) using scattering factors for neutral atoms (Cromer & Mann, 1968) corrected for anomalous dispersion (Cromer & Liberman, 1970). The function $\sum w|KF_o - |F_c||^2$ was minimized where K is a scale factor and w the weight based on counting statistics. Zachariasen's (1963) extinction correction $I_{\text{corr}}=I_{\text{uncorr}}/(1-cI_{\text{uncorr}})$ was applied where c was 0.1×10^{-6} . Reflections for which this correction was greater than 10% and reflections where F_o was less

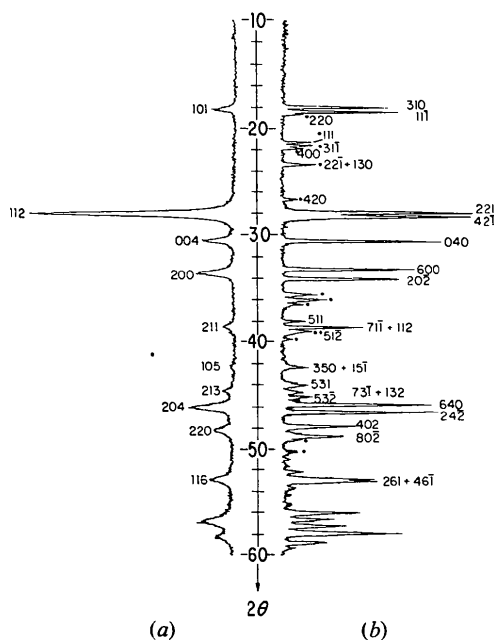


Fig. 1. Diffractometer scans of the disordered (a) and ordered (b) phase of $\text{Bi}_3(\text{FeO}_4)(\text{MoO}_4)_2$ recorded with $\text{Cu K}\alpha$ radiation under comparable conditions. The indices correspond to (a) the basic tetragonal scheelite cell and (b) the large monoclinic cell of the superstructure respectively. Superstructure reflections are indicated by an asterisk.

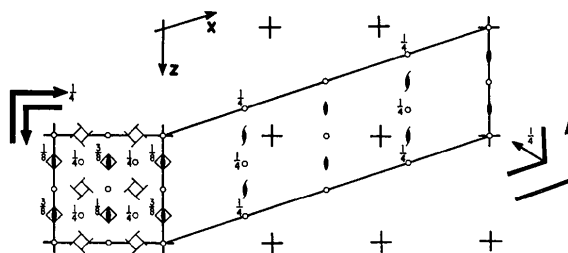


Fig. 2. Relation of the tetragonal scheelite subcell, space group $I4_1/a$, to that of the monoclinic superstructure cell of $\text{Bi}_3(\text{FeO}_4)(\text{MoO}_4)_2$, space group $C2/c$.

than two standard deviations were given zero weight in the final least-squares cycles and are marked with an asterisk in the list of observed and calculated structure factors.* Final positional and thermal parameters are listed in Table 1. The final conventional R value (on F 's) is 0.119 for a total of 1791 reflections, and $R=0.061$ for the 1083 structure factors with nonzero weight in the final refinements. Since these values mainly depend on the agreement of the strong subcell reflections, they cannot be taken as an indicator for the accuracy of the superstructure. However, the R value of 0.034 for the 237 strongest superstructure reflections compares favorably with the R 0.039 for the 108 subcell reflections of the same intensity range.

* A list of structure factors has been deposited with the British Library Lending Division as Supplementary Publication No. SUP 31412 (13 pp., 1 microfiche). Copies may be obtained through The Executive Secretary, International Union of Crystallography, 13 White Friars, Chester CH1 1NZ, England.

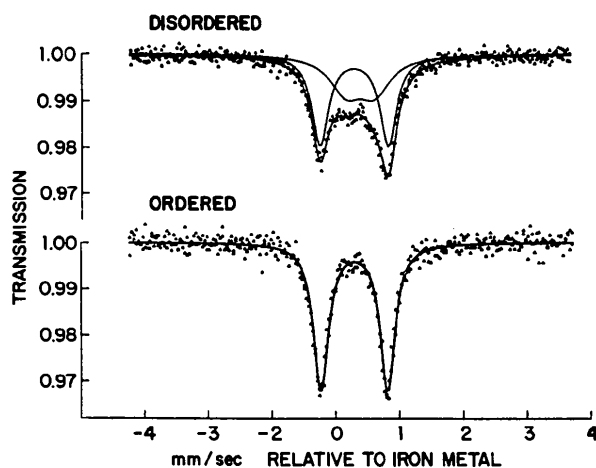


Fig. 3. Least-squares fits to ^{57}Fe Mössbauer spectra of disordered and ordered $\text{Bi}_3(\text{FeO}_4)(\text{MoO}_4)_2$ at 298 K. The data for the ordered phase show an isomer shift $\delta=0.282$ mm s^{-1} and quadrupole splitting $\Delta=1.04$ mm s^{-1} . The data of the disordered phase were fitted arbitrarily to two curves with $\delta_1=0.28$, $\Delta_1=1.06$ mm s^{-1} and $\delta_2=0.39$, $\Delta_2=0.45$ mm s^{-1} . Isomer shifts are given relative to (NBS) $\alpha\text{-Fe}$. Standard deviations are 0.01 mm s^{-1} .

Mössbauer and infrared spectra

In Fig. 3 we compare the ^{57}Fe Mössbauer spectrum of the disordered phase with that of the ordered phase. Experimental details were previously described (Sleight, Chamberland & Weiher, 1968). Only one kind of iron is indicated in the spectrum of the ordered phase and the isomer shift $\delta=0.282$ mm s^{-1} relative to (NBS) $\alpha\text{-Fe}$ is characteristic of high spin Fe^{3+} . The quadrupole splitting of 1.04 mm s^{-1} reflects a significant departure from cubic symmetry.

The isomer shift δ for high spin Fe^{3+} is generally expected to increase with increasing coordination number due to increasing ionicity. For octahedral high-spin Fe^{3+} in oxides, δ is significantly greater than 0.30 mm s^{-1} at room temperature. For tetrahedral high-spin Fe^{3+} , δ is generally in the range of 0.14 to 0.24 mm s^{-1} [see for instance Danon (1968), Birchall & Greenwood (1969)]. Thus the isomer shift for ordered $\text{Bi}_3(\text{FeO}_4)(\text{MoO}_4)_2$ is rather high for high-spin Fe^{3+} in tetrahedral oxygen coordination. It is, however, consistent with the relatively high ionicity and distances of the Fe–O bonds discussed in the next section.

The Mössbauer spectrum of disordered $\text{Bi}_3(\text{FeO}_4)(\text{MoO}_4)_2$ shows the presence of several kinds of iron as would be expected. The fit to two kinds of iron (Fig. 3) is arbitrary but indicates the range of quadrupole splittings and isomer shifts. Relative to the ordered phase there is a trend toward smaller quadrupole splittings and higher isomer shifts. This strongly suggests that some of the iron in disordered $\text{Bi}_3(\text{FeO}_4)(\text{MoO}_4)_2$ has bonding which is even more ionic than in the ordered phase. This could be achieved through a higher coordination number for some of the iron in disordered $\text{Bi}_3(\text{FeO}_4)(\text{MoO}_4)_2$ as is known for the W atom in scheelite-like $\text{Eu}_2(\text{WO}_4)_3$ (Templeton & Zalkin, 1963). On the other hand the isomer shift in the disordered form is certainly not large enough to indicate that Fe occupies the A site of scheelite to any large extent.

Infrared spectra were obtained for ordered and disordered $\text{Bi}_3(\text{FeO}_4)(\text{MoO}_4)_2$ in Nujol mulls (Fig. 4). The peaks shown are primarily due to the MoO_4 groups and the spectra of the two forms are characteristically

Table 1. Atomic parameters in $\text{Bi}_3(\text{FeO}_4)(\text{MoO}_4)_2$

E.s.d.'s are in parentheses in units of the least significant digits. Anisotropic thermal parameters are defined by $\exp[-(\sum h_i h_j b_{ij})]$ and are given $\times 10^3$; equivalent isotropic parameters B are in Å^2 .

	C2/c	x	y	z	b_{11}	b_{22}	b_{33}	b_{12}	b_{13}	b_{23}	B
Bi(1)	8f	0.15163 (6)	0.88676 (9)	0.4058 (2)	76 (3)	112 (7)	845 (33)	2 (4)	42 (7)	20 (12)	0.77 (2)
Bi(2)	4e	0	0.65514 (11)	$\frac{1}{4}$	70 (5)	104 (9)	873 (52)	0	83 (12)	0	0.72 (2)
Fe	4e	0	0.1178 (5)	$\frac{1}{4}$	70 (17)	127 (33)	673 (171)	0	-45 (41)	0	0.77 (7)
Mo	8f	0.16811 (12)	0.3722 (2)	0.4234 (4)	59 (7)	125 (14)	883 (70)	1 (8)	34 (17)	-20 (24)	0.75 (3)
O(1)	8f	0.0870 (11)	0.0394 (16)	0.514 (4)							1.5 (3)
O(2)	8f	0.0510 (11)	0.2015 (15)	0.033 (3)							0.9 (3)
O(3)	8f	0.2173 (12)	0.2888 (16)	0.238 (4)							1.3 (3)
O(4)	8f	0.1161 (11)	0.2912 (15)	0.625 (4)							1.1 (3)
O(5)	8f	0.0919 (10)	0.4531 (15)	0.202 (3)							0.9 (3)
O(6)	8f	0.2459 (10)	0.4586 (15)	0.641 (4)							1.1 (3)

different. In the ordered form all MoO_4 groups are equivalent to each other. However, the MoO_4 groups in disordered $\text{Bi}_3(\text{FeO}_4)(\text{MoO}_4)_2$ will of course not all be equivalent. Furthermore, the symmetry of some molybdate groups in disordered $\text{Bi}_3(\text{FeO}_4)(\text{MoO}_4)_2$ will be lower than for those in ordered $\text{Bi}_3(\text{FeO}_4)(\text{MoO}_4)_2$. Thus the infrared frequencies of the disordered form are less well defined which causes the spectrum to be 'smeared out' relative to that of ordered $\text{Bi}_3(\text{FeO}_4)(\text{MoO}_4)_2$.

Since the vibrational spectra depend primarily on the local environment and symmetry, they are more sensitive to short range order than the X-ray powder patterns. The fact that the bands of the disordered form are broadened considerably, indicates that this form has also considerable disorder at short range. A similar behavior was observed by Schipper & Blasse (1974) for the disordered scheelites $\text{Y}_2(\text{SiO}_4)(\text{WO}_4)$, $\text{Y}_2(\text{GeO}_4)(\text{MoO}_4)$, and $\text{Y}_2(\text{GeO}_4)(\text{WO}_4)$.

Discussion of the ordered structure

The structure of ordered $\text{Bi}_3(\text{FeO}_4)(\text{MoO}_4)_2$ comprises three scheelite-like subcells (Figs. 5 and 6). The tripling of the cell is due to the ordering of the Fe and Mo

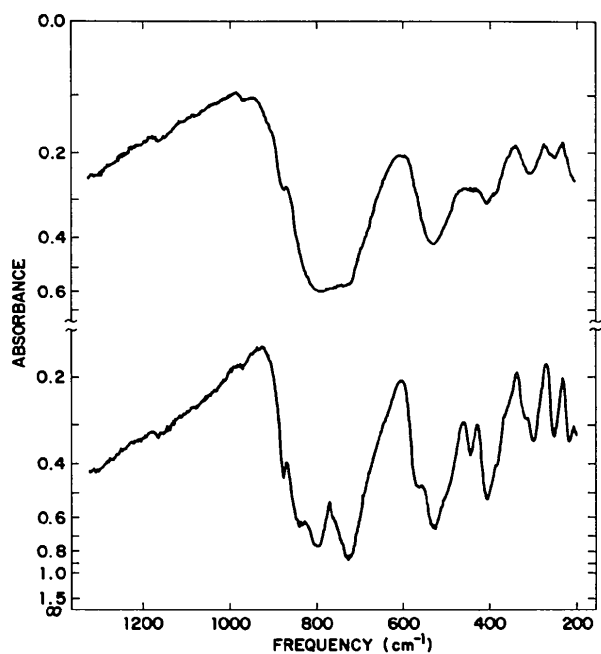


Fig. 4. Infrared absorption spectra of (upper curve) disordered and (lower curve) ordered $\text{Bi}_3(\text{FeO}_4)(\text{MoO}_4)_2$.

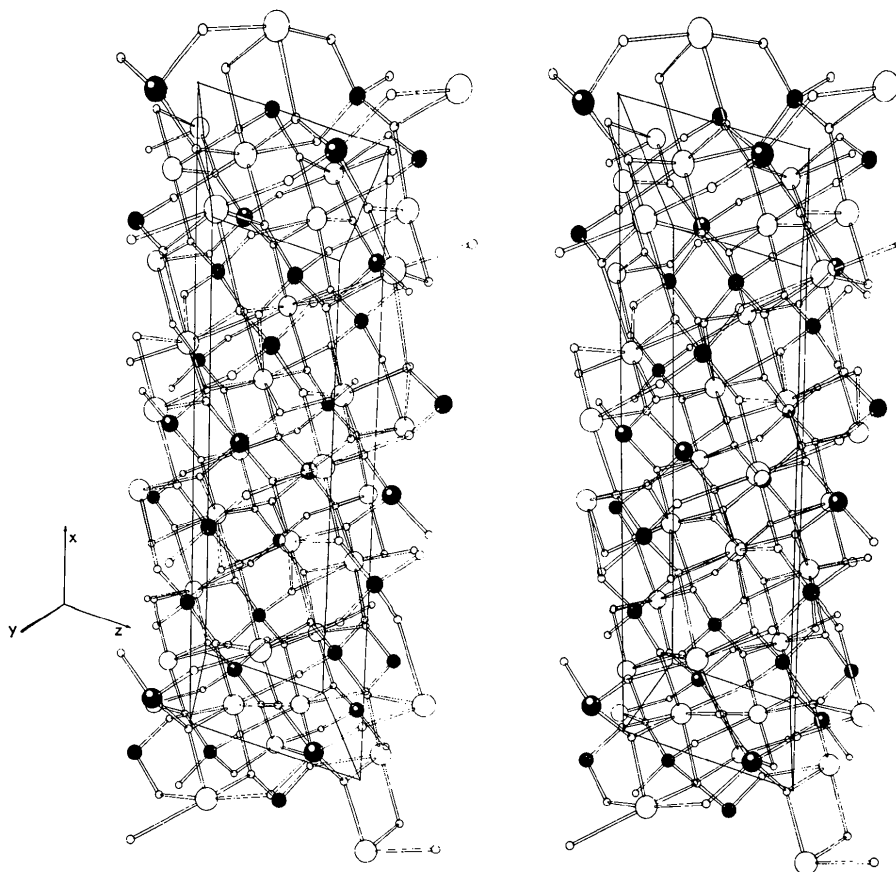


Fig. 5. Stereo drawing of the $\text{Bi}_3(\text{FeO}_4)(\text{MoO}_4)_2$ structure. Bi and O atoms are drawn as large and small white spheres respectively. Black atoms and black atoms with a white dot represent the Mo and Fe atoms.

atoms on the B site of the ABO_4 scheelite structure. The resulting lower symmetry also allows for the characteristic lone-pair distortion in the coordination of the formally 3+ valent Bi atom. Nevertheless both crystallographically different Bi atoms can be considered as eight-coordinate (Fig. 7) which is also the coordination of the A site in scheelite.

The two kinds of Bi atoms are quite different from each other: Bi(1) has three very close O neighbors at about 2.2 Å, while Bi(2) has two very close O neighbors at 2.235 Å and two more at 2.332 Å. The two Bi atoms therefore represent the two most frequently found lone-pair distortions (Brown, 1974) which also occur for Sn^{2+} in the two forms of $SnWO_4$ (Jeitschko & Sleight, 1972, 1974). However, the Bi atoms 'sit' much closer to the centers of the O cages than the Sn atoms. That is, the lone pair of Sn^{2+} has less *s* character than the lone pair of Bi^{3+} , a consequence of the higher stability of the *s* state in the heavier element.

The average Bi–O distances are 2.48₈ Å for Bi(1) and 2.54₃ Å for Bi(2). The difference between these two values is probably due to the larger spread of the Bi(2)–O distances (Table 2). The lengthening of the average bond distance with increasing distortion of the coordination polyhedron is well documented for octahedral MO_6 groups (Brown & Shannon, 1973) and was observed also for P–P distances in polyphosphides (Jeitschko & Donohue, 1975).

The average Fe–O distance of 1.90₈ Å in the tetrahedral FeO_4 group is rather large when compared with the expected distance of 1.85 Å calculated from the Shannon–Prewitt radii. The radius for tetrahedral

Fe^{3+} given by Shannon & Prewitt (1969) was, however, obtained from alkali, earth alkali, and rare-earth ferrites, all ferrites of rather electropositive cations. Bi is less electropositive and because of greater covalency of the short Bi–O bonds, the Fe–O bonds are weakened. This effect of covalency on average interatomic distances was also noted for the Si(Ge)–O bonds in silicates (Noll, 1963) and germanates (Shannon, 1971). Relatively long average Fe–O distances of 1.91₆ for tetrahedral FeO_4 groups were also observed in $BaFe_{12}O_{19}$ (Townes, Fang & Perrotta, 1967). This is consistent with the given rationalization since the O atoms of the FeO_4 tetrahedra in $BaFe_{12}O_{19}$ are linked only to other Fe atoms and not to the (very electropositive) Ba atom.

Thus the relatively high covalency of the Bi–O bonds leads to greater ionicity of the O–Fe bonds and – as noted above – to a relatively large isomer shift. We have searched the literature for tetrahedral Fe^{3+} oxides

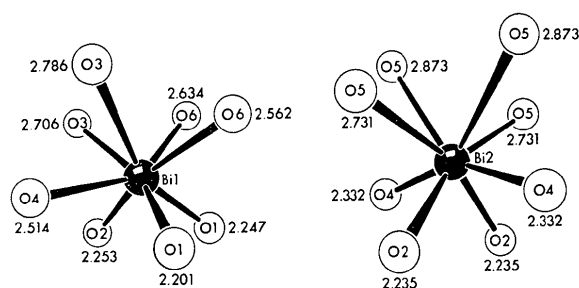


Fig. 7. Near-neighbor coordinations of the Bi atoms in $Bi_3(FeO_4)(MoO_4)_2$. Bi–O distances are indicated in Å.

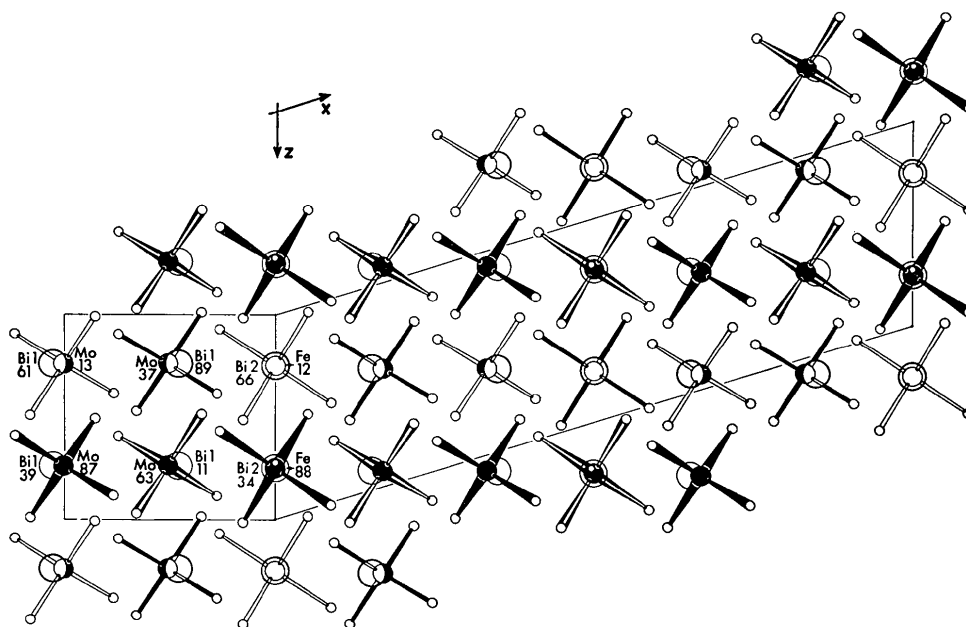


Fig. 6. Projection of the $BiO_3(FeO_4)(MoO_4)_2$ structure. The pseudotetragonal scheelite-like cell is outlined at the left and the correct cell at the right-hand side of the drawing. In the left-hand side of the projection the *y* coordinates of the atoms are given in hundredths. The relative heights of the tetrahedral groups are indicated by different kinds of shading of the metal–oxygen bonds.

Table 2. *Interatomic distances and angles in*
 $\text{Bi}_3(\text{FeO}_4)(\text{MoO}_4)_2$

All metal–oxygen distances shorter than 3.5 Å are given. Standard deviations vary from 0.017 to 0.021 Å and from 0.7 to 1.0°, respectively. There are no O–O distances shorter than 2.78 Å. Of the oxygen–metal–oxygen angles only the tetrahedral angles of the FeO_4 and MoO_4 groups are listed. In the nearly planar OM_3 ‘groups’ (where M are the three nearest neighbors of the oxygens) the Fe–O–Bi angles vary between 117.6 and 129.2°, Mo–O–Bi angles vary between 116.8 and 136.8°, and Bi–O–Bi angles vary between 91.6 and 113.7°.

Bi(1):	O(1)	2.201	O(1):	Fe	1.928
	O(1)	2.247		Bi(1)	2.201
	O(2)	2.253		Bi(1)	2.247
	O(4)	2.514		Fe	2.851
	O(6)	2.562	O(2):	Fe	1.889
	O(6)	2.634		Bi(2)	2.235
	O(3)	2.706		Bi(1)	2.253
	O(3)	2.786		Mo	3.112
Bi(2):	O(2)	2.235 (2 ×)	O(3):	Mo	1.751
	O(4)	2.332 (2 ×)		Bi(1)	2.706
	O(5)	2.731 (2 ×)		Bi(1)	2.786
	O(5)	2.873 (2 ×)		Mo	2.899
Fe:	O(2)	1.889 (2 ×)	O(4):	Mo	1.825
	O(1)	1.928 (2 ×)		Bi(2)	2.332
	O(1)	2.851 (2 ×)		Bi(1)	2.514
	O(4)	3.087 (2 ×)		Fe	3.087
Mo:	O(5)	1.738	O(5):	Mo	1.738
	O(3)	1.751		Bi(2)	2.731
	O(6)	1.779		Bi(2)	2.873
	O(4)	1.825		Mo	3.009
	O(3)	2.899	O(6):	Mo	1.779
	O(6)	2.994		Bi(1)	2.562
	O(5)	3.009		Bi(1)	2.634
	O(2)	3.112		Mo	2.994
O(3)–Mo–O(4)	115.2	O(1)–Fe–O(1)	123.4		
O(3)–Mo–O(5)	107.9	O(1)–Fe–O(2)	101.4 (2 ×)		
O(3)–Mo–O(6)	106.9	O(1)–Fe–O(2)	107.0 (2 ×)		
O(4)–Mo–O(5)	106.3	O(2)–Fe–O(2)	117.8		
O(4)–Mo–O(6)	108.1				
O(5)–Mo–O(6)	112.7				

where both the Fe–O distances and the ^{57}Fe isomer shifts are known with the required accuracy. As anticipated we find (Fig. 8) the ferrite of the most electro-positive ion, $\beta\text{-NaFeO}_2$, at one end and $\text{Bi}_3(\text{FeO}_4)(\text{MoO}_4)_2$ at the other end of the plot.* A direct correlation between the electronegativities of the cations on the one hand and the Fe–O distances and ^{57}Fe isomer shifts on the other hand is not possible, because the actual near-neighbor coordinations would need to be considered, as was discussed above for $\text{BaFe}_{12}\text{O}_{19}$.

Shannon & Vincent (1974) found a high correlation

* Data on spinels $\text{Fe}^{3+}[\text{M}^{2+}\text{M}^{3+}]\text{O}_4$ scatter widely and were excluded because (a) isomer shifts are sometimes quite high, apparently due to small amounts of Fe on the octahedral cation site, and (b) spinels with Fe^{3+} on the tetrahedral site necessarily have cations of two different oxidation states on the octahedral site (indicated by brackets) and therefore only average O positions can be determined which leads to uncertainties in Fe–O distances, especially since some disorder for the tetrahedral site can also be expected.

between a ‘covalency contraction’ parameter and the isomer shift for Fe^{2+} compounds. There the isomer shift varies between 1.45 mm s $^{-1}$ for FeF_2 and 0.55 mm s $^{-1}$ for FeSe . The difference in the isomer shifts of $\beta\text{-NaFeO}_2$ and $\text{Bi}_3(\text{FeO}_4)(\text{MoO}_4)_2$ is much smaller, since here the near-neighbor environment of Fe^{3+} is the same (a more or less distorted tetrahedron of oxygens) and only second-nearest-neighbors (*e.g.*, Na, Bi) vary.

In contrast to the Fe–O distances of the FeO_4 tetrahedra the Mo–O distances of the MoO_4 groups in $\text{Bi}_3(\text{FeO}_4)(\text{MoO}_4)_2$ are much less affected by the presence of the Bi atoms because (a) the O atoms of the MoO_4 tetrahedra do not form short bonds to the Bi atoms and (b) the Mo–O bonds have a Pauling bond strength of 1.5 (*versus* 0.75 for Fe–O) and are therefore less sensitive to small perturbations. Thus, the average Mo–O distance of 1.774 Å in $\text{Bi}_3(\text{FeO}_4)(\text{MoO}_4)_2$ is similar to the tetrahedral Mo–O bond distances of 1.773 Å in Cs_2MoO_4 (Gonschorek & Hahn, 1973), 1.757 Å in $\text{Na}_2\text{Mo}_2\text{O}_7$ (Seleborg, 1967), 1.757 Å in $\beta\text{-Gd}_2(\text{MoO}_4)_3$ (Jeitschko, 1972), and 1.772 Å in $\text{La}_2(\text{MoO}_3)_3$ (Jeitschko, 1973).

Each of the six independent O atoms in $\text{Bi}_3(\text{FeO}_4)(\text{MoO}_4)_2$ is coordinated to two Bi atoms and one tetrahedral (Fe or Mo) atom. Since the oxidation number of Fe is half that of Mo, the formal bond strength of the Fe–O bonds is about half of that of the Mo–O bonds. Thus, to give the same total bond strength to all O atoms, the very short Bi–O bonds are formed by the O atoms of the FeO_4 groups. The O atoms of the MoO_4 groups form long Bi–O bonds. The O(4) atom which forms the shortest Bi–O bond (2.332 Å) of any molybdate O atom, also forms the longest Mo–O bond (1.825 Å). In view of the strong Bi–O and relatively weak Fe–O bonding the formula

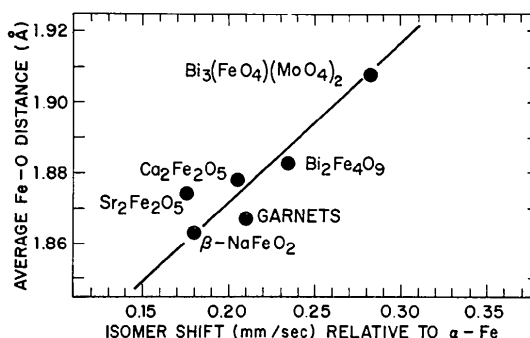


Fig. 8. Isomer shifts and average Fe–O distances in tetrahedral high-spin Fe^{3+} oxides. Structural (first) and Mössbauer data (second reference) were taken from the following papers: $\beta\text{-NaFeO}_2$ (Bertaut, Delapalme & Bassi, 1963; Birchall & Greenwood, 1969), average values for several garnets (Euler & Bruce, 1965; Nicholson & Burns, 1964), $\text{Sr}_2\text{Fe}_2\text{O}_5$ (Greaves, Jacobson, Tofield & Fender, 1975; Gallagher, MacChesney & Buchanan, 1964), $\text{Ca}_2\text{Fe}_2\text{O}_5$ (Colville, 1970; extrapolated from high-temperature data: Geller, Grant & Fullmer, 1970), $\text{Bi}_2\text{Fe}_4\text{O}_9$ (Niizeki & Wachi, 1968; Kostiner & Shoemaker, 1971), $\text{Bi}_3(\text{FeO}_4)(\text{MoO}_4)_2$ (this work).

could be written $\text{Fe}(\text{Bi}_3\text{O}_4)(\text{MoO}_4)_2$. This formulation, however, obscures the close relation to scheelite.

Disordered and ordered $\text{Bi}_3(\text{GaO}_4)(\text{MoO}_4)_2$

We have prepared $\text{Bi}_3(\text{GaO}_4)(\text{MoO}_4)_2$ as described above for the iron compound, substituting gallium nitrate for ferric nitrate. Our results are analogous to those for $\text{Bi}_3(\text{FeO}_4)(\text{MoO}_4)_2$. When heated to only 250°C the X-ray powder diagrams show only the broad lines characteristic for the tetragonal scheelite type cell ($a = 5.31, c = 11.67 \text{ \AA}$). After heating at 700°C for 10 h the scheelite subcell lines are split and superstructure lines are present. A Hagg-Guinier pattern was indexed with the cell corresponding to that of ordered $\text{Bi}_3(\text{FeO}_4)(\text{MoO}_4)_2$. The least-squares refined lattice constants are: $a = 16.863 (2), b = 11.665 (1), c = 5.227 (1) \text{ \AA}, \beta = 107.23 (1)^\circ, V = 980.4 (1) \text{ \AA}^3$. We have calculated the powder pattern for ordered $\text{Bi}_3(\text{GaO}_4)(\text{MoO}_4)_2$ using the positional parameters of Table 1. The good agreement in calculated and observed d -spacings and intensities (Table 3) confirms that ordered $\text{Bi}_3(\text{GaO}_4)(\text{MoO}_4)_2$ has the same structure as ordered $\text{Bi}_3(\text{FeO}_4)(\text{MoO}_4)_2$. The color of the two $\text{Bi}_3(\text{GaO}_4)(\text{MoO}_4)_2$ modifications is a very light yellow, almost white.

Table 3. Evaluation of the low-angle lines of a Hagg-Guinier pattern of ordered $\text{Bi}_3(\text{GaO}_4)(\text{MoO}_4)_2$

Cu $K\alpha_1$ radiation; calculated data were generated by a computer program (Yvon, Jeitschko & Parthé, 1969).

hk l^*	hk l	d_o	d_c	I_o	I_c	hk l^*	hk l	d_o	d_c	I_o	I_c
11 0	9.847	9.832	5	w	15 0	2.3089	2.3072	3	vw		
20 0	6.055	8.034	1	vw	24 1	2.3072	2	vw			
02 0	5.932	-	<1	-	02 2	2.2949	2.2949	1	vw		
31 0	4.877	4.870	15	m	44-1	2.2947	-	-	-		
11-1	4.769	4.767	19	m	51-2	2.2930	-	-	-		
22 0	4.725	4.719	3	vw	42-2	2.2755	-	-	-		
11 1	4.127	4.119	1	w	71 0	2.2574	2.2559	1	vw		
31-1	4.080	4.083	4	w	20 2	2.2066	2.2045	<1	vw		
40 0	4.026	4.020	3	w	60-2	2.1778	2.1798	1	vw		
02 1	3.792	-	1	-	13-2	2.1559	-	-	-		
13 0	3.779	-	2	-	33-2	2.1401	-	-	-		
22-1	3.774	3.777	2	w	35 0	2.1397	2.1405	2	vw		
42 0	3.515	3.509	9	vw	15-1	2.1304	2.1309	3	vw		
22 1	3.167	3.163	100	vw	22 2	2.0658	-	-	-		
33 0	3.1492	-	8	-	15 1	2.0625	2.0609	1	vw		
42-1	3.1353	3.1362	95	vw	35-1	2.0566	-	-	-		
13-1	3.1197	3.1218	3	vw	33 1	2.0455	2.0420	3	w		
51 0	3.1050	3.1024	2	vw	31 2	2.0135	-	-	-		
31 1	3.0959	-	<1	-	73-1	2.0262	-	-	-		
51-1	3.0510	-	<1	-	13 2	2.0194	2.0182	2	vw		
13 1	2.9175	-	<1	-	80 0	2.0133	2.0116	3	w		
04 0	2.9153	2.9175	<1	-	31 2	2.0135	-	-	-		
33-1	2.9006	-	<1	-	44 1	2.0046	-	-	-		
2 0	2.7420	-	<1	-	53-2	2.0027	2.0049	4	w		
200	2.6844	2.6921	21	m	64-1	1.9910	-	-	-		
20-2	2.6132	2.6138	23	m	62 0	1.9901	-	-	-		
11-2	2.5841	-	<1	-	71-2	1.9858	-	-	-		
04 1	2.5181	-	3	-	73 0	1.9902	-	-	-		
31-2	2.5132	2.5161	<1	-	64 0	1.9750	1.9749	25	vw		
24-1	2.5187	-	1	w	62-1	1.9735	-	-	-		
00 2	2.4962	-	<1	-	24-2	1.9462	1.9459	28	vw		
42 1	2.4949	2.4904	1	vw	06 0	1.9442	-	-	-		
53 0	2.4806	2.4739	3	w	82 0	1.9031	-	-	-		
33 1	2.4764	2.4726	3	w	04 2	1.8964	-	-	-		
40-2	2.4752	-	<1	-	26 0	1.8599	-	-	-		
1 0	2.4687	-	1	w	55 0	1.8895	-	-	-		
53-1	2.4559	2.4574	3	vw	35 1	1.8877	-	-	-		
60 0	2.4395	-	<1	-	44-2	1.8971	-	-	-		
22-2	2.3849	-	<1	-	40 2	1.8861	1.8842	13	m		
44 0	2.3619	2.3619	2	vw	95-1	1.8789	-	-	-		
51 1	2.3526	-	1	w	71 1	1.8636	-	-	-		
71-1	2.3393	2.3275	6	vw	80-2	1.8591	1.8602	13	m		
11 2	2.3161	2.3127	7	m	91-1	1.8451	-	-	-		

* Indices of scheelite-like subcell

Crystal chemistry of scheelites

In Fig. 9 we show some of the better established scheelite-related structures and their space-group rela-

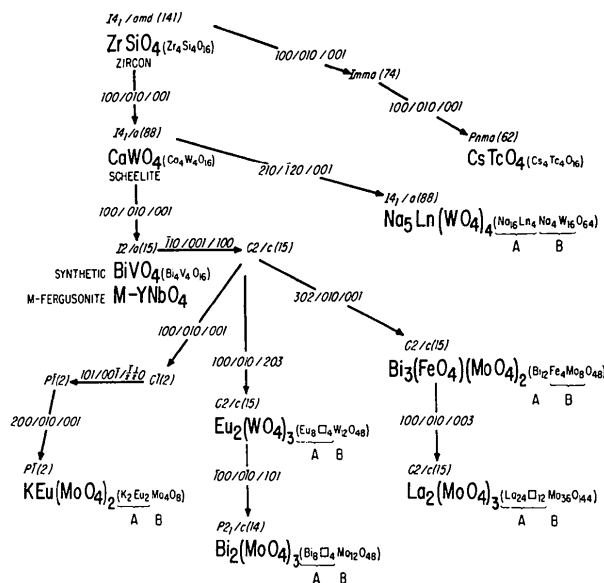


Fig. 9. Structural and space-group relationships of scheelite-related phases. Chemical formulas in parentheses indicate the content of the cell. Vacant sites are indicated by squares. The number of the space group is given in parentheses behind the Hermann-Mauguin symbol. The transformation matrices are also shown. They correspond to the monoclinic settings with the b axis unique.

tionships. Besides the compounds already mentioned in the introduction, this scheme contains also the $\text{Na}_5\text{Ln}(\text{WO}_4)_4$ structure (Ln =rare earth) where one-fifth of the WO_4 groups is replaced by Na (Sillén & Sundvall, 1943; Klevtsova, Glinskaya, Kozeeva & Klevtsov, 1973; Hong & Dwight, 1974).

M -Fergusonite, M - YNbO_4 , derives from a scheelite type structure by a displacive phase transition (Wolton & Chase, 1967). The crystal structure of this phase was described in the non-centrosymmetric space group $C2$ (Komkov, 1959) although systematic absences indicated space groups $1a(Cc)$ or $I2/a(C2/c)$. We have prepared the compounds $\text{YNbO}_4, \text{YTaO}_4, \text{LaNbO}_4$, and NdTaO_4 from high-purity oxides (except for LaNbO_4 where $\text{La}(\text{OH})_3$ was used) fired at 1700 K for 2 h, grinding, followed by annealing at 1700 K for 12 h and quenched. They show an X-ray powder pattern as reported in the ASTM data file for the distorted scheelite structure. Their second harmonic generation signal (Kurtz & Perry, 1968), however, was so small (much less than one tenth that of quartz) that we attribute it to impurity effects. For that reason we ascribe the centric space group $I2/a(C2/c)$ to these compounds, as was done also for synthetic BiVO_4 (Bierlein & Sleight, 1975). In all these structures the positions and orientations of the tetrahedral BO_4 groups are the same as in scheelite.*

* The cell dimensions of M' -fergusonite, M' - YTaO_4 (Wolten, 1967) and the mineral pucherite, BiVO_4 (Qurashi & Barnes, 1953) are similar to those of scheelite, but the metal positions are very different. Thus in terms of space-group relationships they cannot be described as scheelite related.

The locations of the tetrahedral groups of the zircon (ZrSiO_4) structure are the same as in scheelite, but their orientation is different. The cell dimensions and metal positions of CsTcO_4 (Meyer & Hoppe, 1976) are similar to scheelite, but the orientations of the tetrahedral groups correspond to those of the zircon structure.

$\text{KBi}(\text{MoO}_4)_2$ (Klevtsov & Vinokurov, 1975), $\text{KLn}(\text{WO}_4)_2$ ($\text{Ln}=\text{Sm}$ to Tb ; Klevtsov, Kozeeva, Kharchenko & Pavlyuk, 1974), and $\text{Na}_2\text{Th}(\text{WO}_4)_3$ (Trunov & Bushuev, 1969) are scheelite-related, but their space groups and exact structures are not yet known.

We are indebted to D. M. Graham for competent help with the crystallographic work.

References

- BERTAUT, F., DELAPALME, A. & BASSI, G. (1963). *C. R. Acad. Sci. Paris*, **257**, 421–424.
- BIERLEIN, J. D. & SLEIGHT, A. W. (1975). *Solid State Commun.* **16**, 69–70.
- BIRCHALL, T. & GREENWOOD, N. N. (1969). *J. Chem. Soc. (A)*, pp. 2382–2398.
- BRIXNER, L. H., SLEIGHT, A. W. & LICIS, M. S. (1972). *J. Solid State Chem.* **5**, 247–249.
- BROWN, I. D. (1974). *J. Solid State Chem.* **11**, 214–233.
- BROWN, I. D. & SHANNON, R. D. (1973). *Acta Cryst.* **A29**, 266–282.
- CESARI, M., PEREGO, G., ZAZZETTA, A., MANARA, G. & NOTARI, B. (1971). *J. Inorg. Nucl. Chem.* **33**, 3595–3597.
- COLVILLE, A. A. (1970). *Acta Cryst.* **B26**, 1469–1473.
- CROMER, D. T. & LIBERMAN, D. (1970). *J. Chem. Phys.* **53**, 1891–1898.
- CROMER, D. T. & MANN, J. B. (1968). *Acta Cryst.* **A24**, 321–324.
- DANON, J. (1968). In *Chemical Applications of Mössbauer Spectroscopy*, edited by V. I. GOLDANSKII & R. H. HERBER. New York, London: Academic Press.
- ELZEN, A. F. VAN DEN & RIECK, G. D. (1973). *Acta Cryst.* **B29**, 2433–2436.
- EULER, F. & BRUCE, J. A. (1965). *Acta Cryst.* **19**, 971–978.
- FINGER, L. W. (1969). Unpublished computer program for the least-squares refinement of crystal structures.
- GALLAGHER, P. K., MACCHESNEY, J. B. & BUCHANAN, D. N. E. (1964). *J. Chem. Phys.* **41**, 2429–2434.
- GELLER, S., GRANT, R. W. & FULLMER, L. D. (1970). *J. Phys. Chem. Solids*, **31**, 793–803.
- GONSHOREK, W. & HAHN, T. (1973). *Z. Kristallogr.* **138**, 167–176.
- GREAVES, C., JACOBSON, A. J., TOFIELD, B. C. & FENDER, B. E. F. (1975). *Acta Cryst.* **B31**, 641–646.
- HONG, H. Y-P. & DWIGHT, K. (1974). *Mater. Res. Bull.* **9**, 775–780.
- JEITSCHKO, W. (1972). *Acta Cryst.* **B28**, 60–76.
- JEITSCHKO, W. (1973). *Acta Cryst.* **B29**, 2074–2081.
- JEITSCHKO, W. & DONOHUE, P. C. (1975). *Acta Cryst.* **B31**, 574–580.
- JEITSCHKO, W. & SLEIGHT, A. W. (1972). *Acta Cryst.* **B28**, 3174–3178.
- JEITSCHKO, W. & SLEIGHT, A. W. (1974). *Acta Cryst.* **B30**, 2088–2094.
- KLEVTSOV, P. V., KOZEEVA, L. P., KHARCHENKO, L. YU. & PAVLYUK, A. A. (1974). *Sov. Phys. Crystallogr.* **19**, 342–345.
- KLEVTSOV, P. V. & VINOKUROV, V. A. (1975). *Sov. Phys. Crystallogr.* **19**, 474–476.
- KLEVTSOVA, R. F., GLINSKAYA, L. A., KOZEEVA, L. P. & KLEVTSOV, P. V. (1973). *Sov. Phys. Crystallogr.* **17**, 672–676.
- KLEVTSOVA, R. F., KOZEEVA, L. P. & KLEVTSOV, P. V. (1974). *Sov. Phys. Crystallogr.* **19**, 50–53.
- KOMKOV, A. I. (1959). *Sov. Phys. Crystallogr.* **4**, 796–800.
- KOSTINER, E. & SHOEMAKER, G. L. (1971). *J. Solid State Chem.* **3**, 186–189.
- KURTZ, S. K. & PERRY, T. T. (1968). *J. Appl. Phys.* **39**, 3798–3813.
- LINN, W. J. & SLEIGHT, A. W. (1976). *J. Catal.* In the press.
- MEYER, G. & HOPPE, R. (1976). *Z. anorg. allgem. Chem.* In the press.
- MULLER, O. & ROY, R. (1974). *Major Ternary Structural Families*. Berlin, Heidelberg, New York: Springer.
- NICHOLSON, W. J. & BURNS, G. (1964). *Phys. Rev.* **133**, A1568–A1570.
- NIIZEKI, N. & WACHI, M. (1968). *Z. Kristallogr.* **127**, 173–187.
- NOLL, W. (1963). *Angew. Chem. Int. Ed.* **2**, 73–80.
- QURASHI, M. M. & BARNES, W. H. (1953). *Amer. Min.* **38**, 489–500.
- SCHIPPER, W. J. & BLASSE, G. (1974). *Z. Naturforsch.* **29b**, 340–346.
- SELEBORG, M. (1967). *Acta Chem. Scand.* **21**, 499–504.
- SHANNON, R. D. (1971). *Chem. Commun.* pp. 881–882.
- SHANNON, R. D. & PREWITT, C. T. (1969). *Acta Cryst.* **B25**, 925–946.
- SHANNON, R. D. & VINCENT, H. (1974). *Struct. Bond.* **19**, 1–43.
- SILLÉN, L. G. & SUNDVALL, H. (1943). *Ark. Kem. Miner. Geol.* **17A**, (10), 1–18.
- SLEIGHT, A. W., CHAMBERLAND, B. L. & WEIHER, J. F. (1968). *Inorg. Chem.* **7**, 1093–1098.
- SLEIGHT, A. W. & JEITSCHKO, W. (1974). *Mater. Res. Bull.* **9**, 951–954.
- TEMPLETON, D. H. & ZALKIN, A. (1963). *Acta Cryst.* **16**, 762–766.
- TOWNES, W. D., FANG, J. H. & PERROTTA, A. J. (1967). *Z. Kristallogr.* **125**, 437–449.
- TRUNOV, V. K. & BUSHUEV, N. N. (1969). *Radiokhimiya*, **11**, 245–247.
- WEBER, K. (1969). *Acta Cryst.* **B25**, 1174–1178.
- WOLTEN, G. M. (1967). *Acta Cryst.* **23**, 939–944.
- WOLTEN, G. M. & CHASE, A. B. (1967). *Amer. Min.* **52**, 1536–1541.
- YVON, K., JEITSCHKO, W. & PARTHÉ, E. (1969). *A Fortran IV Program for the Intensity Calculation of Powder Patterns*. Report of the LRSM Laboratory, Univ. of Pennsylvania, Philadelphia, Pa.
- ZACHARIASEN, W. H. (1963). *Acta Cryst.* **16**, 1139–1144.